

# Design and production of bicolour reflecting coatings with Au metal island films

Vesna Janicki,<sup>1,\*</sup> Tatiana V. Amotchkina,<sup>2</sup> Jordi Sancho-Parramon,<sup>1</sup> H. Zorc,<sup>1</sup> Michael K. Trubetskov,<sup>2</sup> and Alexander V. Tikhonravov<sup>2</sup>

<sup>1</sup>Department LARD, Ruđer Bošković Institute, Bijenička c. 54, 10000 Zagreb, Croatia

<sup>2</sup>Research Computing Center, Moscow State University, Leninskie Gory, 199992 Moscow, Russia  
[janicki@irb.hr](mailto:janicki@irb.hr)

**Abstract:** Optical properties of metal island films (MIFs) can be combined with interference of dielectric coatings. A set of multilayer designs containing metal clusters reflecting different colours from front and back side of the coating was obtained by numerical optimization. The chosen designs presenting the range of feasible colours were deposited by electron beam evaporation. Spectrophotometric and ellipsometric measurements verified that the produced coatings present an excellent agreement with the optical performance calculated from the designs. Numerical optimization was verified as a useful method in designing of coatings containing MIFs. This approach can ease the implementation of metal clusters into multilayer designs and broaden the applications of MIFs.

©2011 Optical Society of America

**OCIS codes:** (160.4670) Optical materials; (230.4170) Multilayers; (240.6680) Surface plasmons; (310.3915) Metallic, opaque, and absorbing coatings; (310.4165) Multilayer design.

---

## References and links

1. U. Kreibig and M. Vollmer, *Optical Properties of Metal Clusters* (Springer, Berlin, 1995).
2. S. Kachan, O. Stenzel, and A. Ponyavina, "High-absorbing gradient multilayer coatings with silver nanoparticles," *Appl. Phys. B* **84**(1-2), 281–287 (2006).
3. W. Gotschy, K. Vonmetz, A. Leitner, and F. R. Aussenegg, "Optical dichroism of lithographically designed silver nanoparticle films," *Opt. Lett.* **21**(15), 1099–1101 (1996).
4. J.-N. Yih, W.-C. Hsu, S.-Y. Tsai, and S.-J. Chen, "Enhanced readout signal of superresolution near-field structure disks by control of the size and distribution of metal nanoclusters," *Appl. Opt.* **44**(15), 3001–3005 (2005).
5. M. Lahav, A. Vaskevich, and I. Rubinstein, "Biological sensing using transmission surface plasmon resonance spectroscopy," *Langmuir* **20**(18), 7365–7367 (2004).
6. G. D. Sockalingum, A. Beljebbar, H. Morjani, J. F. Angiboust, and M. Manfait, "Characterization of island films as surface-enhanced Raman spectroscopy substrates for detecting low antitumor drug concentrations at single cell level," *Biospectroscopy* **4**(S5), S71–S78 (1998).
7. P. Heger, O. Stenzel, and N. Kaiser, "Metal island films for optics," *Proc. SPIE* **5250**, 21–28 (2004).
8. S. Husaini, L. Deych, and V. M. Menon, "Plasmon-resonance-induced enhancement of the reflection band in a one-dimensional metal nanocomposite photonic crystal," *Opt. Lett.* **36**(8), 1368–1370 (2011).
9. V. Janicki, J. Sancho-Parramon, and H. Zorc, "Gradient silver nanoparticle layers in absorbing coatings-experimental study," *Appl. Opt.* **50**(9), C228–C231 (2011).
10. M. Hövel, B. Gompf, and M. Dressel, "Dielectric properties of ultrathin metal films around the percolation threshold," *Phys. Rev. B* **81**(3), 035402 (2010).
11. A. J. de Vries, E. S. Kooij, H. Wormeester, A. A. Mewe, and B. Poelsema, "Ellipsometric study of percolation in electroless deposited silver films," *J. Appl. Phys.* **101**(5), 053703 (2007).
12. J. Sancho-Parramon, V. Janicki, and H. Zorc, "On the dielectric function tuning of random metal-dielectric nanocomposites for metamaterial applications," *Opt. Express* **18**(26), 26915–26928 (2010).
13. J. Sancho-Parramon, V. Janicki, and H. Zorc, "Tuning the effective dielectric function of thin film metal-dielectric composites by controlling the deposition temperature," *J. Nanophotonics* **5**(1), 051805/1–051805/8 (2011).
14. J. Bulíř, M. Novotný, A. Lunnykova, and J. Lančok, "Preparation of nanostructured ultrathin silver layer," *J. Nanophotonics* **5**, 051511/1–051511/10 (2011).
15. T. V. Amotchkina, V. Janicki, J. Sancho-Parramon, A. V. Tikhonravov, M. K. Trubetskov, and H. Zorc, "General approach to reliable characterization of thin metal films," *Appl. Opt.* **50**(10), 1453–1464 (2011).
16. T. V. Amotchkina, M. K. Trubetskov, A. V. Tikhonravov, V. Janicki, J. Sancho-Parramon, and H. Zorc, "Reliable characterization of thin metal-dielectric films," *Appl. Opt.* (to be published).

17. J. A. Dobrowolski, S. Browning, M. Jacobson, and M. Nadal, "2007 topical meeting on optical interference coatings: manufacturing problem," *Appl. Opt.* **47**(13), C231–C245 (2008).
  18. U. Beckers, O. Stenzel, S. Wilbrandt, U. Falke, and C. von Borczyskowski, "The optical absorption of ultrathin organic molecular films: the thickness dependence of the absorption line position," *J. Phys. Condens. Matter* **10**(8), 1721–1732 (1998).
  19. E. D. Palik, *Handbook of Optical Constants of Solids* (Academic Press, 1985).
  20. T. V. Amotchkina, J. Sancho-Parramon, V. Janicki, M. K. Trubetskov, H. Zorc, and A. V. Tikhonravov, "Design of multilayer coatings containing metal island films," presented at SPIE Optical System Design 2011, paper 8168–8, Marseille, France, 5–8 2011.
  21. R. W. G. Hunt, *Measuring colours* (Fountain Press, London, 1998).
  22. A. V. Tikhonravov and M. K. Trubetskov, "OptiLayer thin film software," <http://www.optilayer.com>
- 

## 1. Introduction

Metal clusters attract a lot of interest due to surface plasmon resonance (SPR) of free electrons, presenting a strong absorption at specific wavelengths that depend on the particle size, shape, spatial distribution and dielectric environment [1]. They are used in selective absorbers, data storage [2–4], or in chemical and biological sensing and surface enhanced spectroscopy [5, 6].

Combining SPR of metal clusters in a film, such as a metal island film (MIF), and interference of dielectric coatings, it is possible to get even more sophisticated optical properties of multilayer systems than employing only absorption or only interference properties [7–9]. MIF can be easily produced using standard thin film equipment.

In the case of dielectric coatings, the designs are obtained by numerical optimization of optical properties of the model, according to the desired properties defined as a target. In this process, optimization parameters are typically layer thicknesses and the assignments of layer materials to layers. The number of design layers can also vary within some reasonable limits. The designs containing metal clusters are very often constructed from MIFs and quarter wave layers, in order to enhance reflectance ( $R$ ) or absorption ( $A$ ) at a specific wavelength [2,8]. This approach is sometimes lacking the final refinement of the thicknesses that could improve the performance and adjust it to a more sophisticated target.

If the metal clusters are small compared to the wavelength of the incidence light, it is possible to describe their optical behaviour using effective optical constants and thickness that can be determined from experimental measurements [10–14]. The effective optical constants in the visible range are governed by the SPR, with a strong absorption peak and the associated dispersion of refractive index. Therefore, the wavelength dependence of the optical constants of MIFs is quite different from the one of classical dielectrics and metals typically used in design and production of optical coatings. Thus, the incorporation of MIFs in optical coatings could enable new performance possibilities. Nevertheless, one has to keep in mind that optical constants of MIFs are strongly dependent on thickness [12]. It is necessary to take this dependence into account in the design process in order to fully integrate MIFs in numerical optimization [15, 16].

In this paper we present multilayer coatings containing MIFs that are successfully deposited based on the design obtained by numerical optimization to the desired targets. We chose to make systems that reflect different colours from front and back side of the coating. This requirement cannot be fulfilled using dielectric layers only, since reflectance of different colours from each side requires the use of absorbing layers [17]. Although in this work we did not specify the desired transmittance output, the use of metal layers, generally speaking, could limit the transmittance of the coating due to high absorbance. One has to keep in mind that growing of very thin metal layer is technically difficult task. The advantage of MIFs, compared with compact metal layers, is lower absorbance and therefore larger attainable transmittance. Also, the absorption peak of SPR can be easily tuned by changing the dielectric environment. The realized excellent agreement between design and experimental data confirms that MIFs can be incorporated into the design and production of optical coatings, enabling achieving targets that are not accessible using only classical dielectric and metal coatings.

## 2. Design

Optical properties of Au MIFs remain stable upon exposure to atmospheric conditions, so this was our motivation to use gold. Prior to the design of multilayer system containing metal clusters, it is necessary to know how optical constants of MIF change with thickness. For this purpose a set of Au MIFs with different thicknesses embedded in a dielectric matrix was deposited on the pre-heated substrates. The thickness of the surrounding dielectric layers was the same for all samples. The dielectric layer had to be thick enough to cover metal clusters completely, so they could be treated in the design as an effectively homogeneous layer. Also, it had to be thick enough to prevent an influence of another dielectric material that could change the dielectric environment of the metal clusters [18]. Spectrophotometric and ellipsometric measurements of these samples were performed and their effective optical constants and thickness determined. Au MIFs obtained in such a way show strong absorption related to SPR at wavelengths 500-700 nm [16]. As an example, the optical constants of Au MIF of 17.6 nm thickness in SiO<sub>2</sub> matrix are presented in Fig. 1, where they are compared with constants of bulk Au [19].

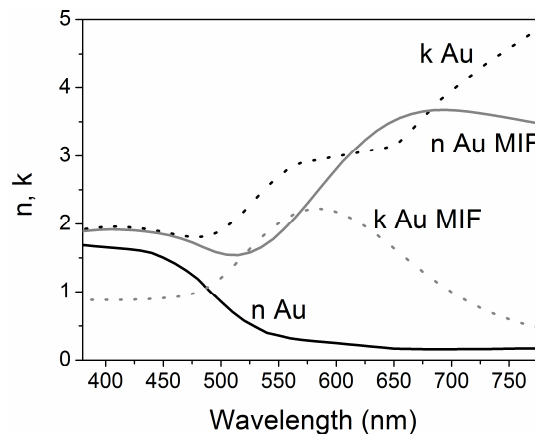


Fig. 1. Optical constants of Au MIF of 17.6 nm thickness and bulk Au [19] are shown together for comparison.

Before starting with the design process, one has to keep in mind constraints to optimization parameters that are imposed by implementation of MIFs. The thickness of the MIFs in the designs is constrained below percolation limit when deposited onto a pre-heated substrate. In this case, optical characteristics of MIFs are dominated by SPR, showing dielectric behaviour. As the amount of metal increases, percolation among islands starts and the metal-like behaviour characterized by strong infrared absorption becomes evident in the effective optical constants [16]. Since optical constants of metal clusters depend on the environment, MIF always has to be embedded into the same dielectric as for the test samples. From the practical point of view, this means that MIFs have to be included into the design as dielectric/MIF/dielectric. For example, if the needle method is used, this structure has to remain locked for introduction of new materials [20]. The minimal thickness of embedding dielectric layers has to be the same as their thickness in the test.

The aim was to obtain designs that would reflect clearly different specified colours from front and back side of the coating. This requirement had to be fulfilled for angles of incidence (AOI) 0-30°. The target colours were defined as chromaticities according to CIE 1931 Standard Observer colour coordinate system [21]: violet ( $x = 0.2, y = 0.1$ ), green ( $x = 0.25, y = 0.5$ ), yellow ( $x = 0.4, y = 0.5$ ), orange ( $x = 0.5, y = 0.4$ ), and red ( $x = 0.6, y = 0.3$ ). All these requirements were imposed into OptiLayer thin film software [22] prior to the design procedure.

In order to estimate closeness between theoretical and target color characteristics we introduced the merit function:

$$F = \sqrt{(x_{R_a} - \hat{x}_{R_a})^2 + (y_{R_a} - \hat{y}_{R_a})^2 + (x_{R_b} - \hat{x}_{R_b})^2 + (y_{R_b} - \hat{y}_{R_b})^2} \quad (1)$$

where  $(x_{R_a}, y_{R_a})$ ,  $(x_{R_b}, y_{R_b})$  are chromaticities of the light reflected from the front and back side of the sample,  $(\hat{x}_{R_a}, \hat{y}_{R_a})$ ,  $(\hat{x}_{R_b}, \hat{y}_{R_b})$  are the target chromaticities. More details about the design procedure and design algorithm based on the minimization of merit function (Eq. (1)) are given in ref [20].

The designs with an Au MIF layer of thickness 15-19 nm represent a good balance between the requirement for saturation of colours and being far from percolation limit. The designs having thinner MIFs do not show enough absorption to make clear difference in colours reflected from front and back side. Different optical constants for MIFs of different thicknesses are taken into account in the design.

From the set of the obtained designs we chose for deposition those that have minimal number of layers (4-7) and that are less sensitive to thickness errors. Regarding the colours, we were choosing designs with more contrasted colours reflected from the two sides. Thus, combinations like violet-magenta or orange-yellow did not look interesting. The design TAD91 that gives green-yellow combination was chosen as a representative of multilayers containing Au MIF embedded in TiO<sub>2</sub>, contrary to SiO<sub>2</sub> in the other chosen designs. Due to the higher dielectric constant of TiO<sub>2</sub> compared with SiO<sub>2</sub>, SPR in TiO<sub>2</sub> is red-shifted. The structures of the designs presenting a variety of achievable colours are presented in Table 1. The first and second colour describing the design are colours reflected from the front and back side of the coating, respectively. The uppermost row corresponds to the layer next to the substrate.

**Table 1. Designs chosen for deposition.**

TAD32 violet-yellow		TAD7a violet-orange		TAD7b magenta-yellow		TAD8b orange-green		TAD91 green-yellow	
Material	Thickness (nm)	Material	Thickness (nm)	Material	Thickness (nm)	Material	Thickness (nm)	Material	Thickness (nm)
SiO <sub>2</sub>	85.8	TiO <sub>2</sub>	92.7	TiO <sub>2</sub>	92.7	SiO <sub>2</sub>	103.1	TiO <sub>2</sub>	110
Au MIF	17.6	SiO <sub>2</sub>	101.4	SiO <sub>2</sub>	100.5	Au MIF	17.6	Au MIF	19.5
SiO <sub>2</sub>	224.3	Au MIF	15.4	Au MIF	16.3	SiO <sub>2</sub>	148.1	TiO <sub>2</sub>	207.8
TiO <sub>2</sub>	25.1	SiO <sub>2</sub>	79.7	SiO <sub>2</sub>	79.8	TiO <sub>2</sub>	59.7	SiO <sub>2</sub>	50.9
		TiO <sub>2</sub>	25.2	TiO <sub>2</sub>	14.8	SiO <sub>2</sub>	100.9	TiO <sub>2</sub>	32.1
		SiO <sub>2</sub>	85.2	SiO <sub>2</sub>	27.7	TiO <sub>2</sub>	77.8	SiO <sub>2</sub>	42.7
		TiO <sub>2</sub>	26.8	TiO <sub>2</sub>	89.2			TiO <sub>2</sub>	18.1

### 3. Experimental

The multilayer structures containing metal clusters embedded in a dielectric matrix were prepared by the sequential electron beam evaporation of the materials in a modified Varian deposition chamber. The base pressure was 10<sup>-6</sup> torr. The substrates were 1 mm thick N-BK7 chips. The layer mass thickness was controlled by a quartz crystal monitor. Deposition rates were around 1 Å/s for Au and 10 Å/s for SiO<sub>2</sub> and TiO<sub>2</sub>. The substrates were pre-heated to 220°C.

The measurements of the optical performance of the samples at normal incidence were done by a Perkin Elmer Lambda 25 spectrophotometer. Reflectance and transmittance measurements were performed in the range 380–780 nm. The measurements of reflectance at non-normal incidence were done using a Woollam V-VASE ellipsometer.

### 4. Results and discussion

The performance of the samples reflecting different colours from the two sides is presented in Fig. 2 where photographs of reflected light from all the samples are shown. One can see that the required colours were clearly realized. However, since it is difficult to reproduce the true

colours because of the limitations of the media (camera, printer or screen), these photographs are presented only for the purpose that the reader gets an idea of the obtained performance.



Fig. 2. Photographs of the samples reflection from the front side (above) and back side (below). Numbers 1, 2, 3, 4 and 5 correspond to samples TAD32, TAD7a, TAD7b, TAD8b and TAD91, respectively.

Table 2 presents a more objective approach to present the results. The colour chromaticities of the coatings are compared with the target colours in Table 2. One can see that the requirements are very well matched. Spectrophotometric measurements of the light reflected from front ( $R_a$ ) and back ( $R_b$ ) side of the samples, together with their transmittance ( $T$ ) are compared with the theoretical values calculated from the designs in Fig. 3. The total losses of the measured spectra ( $L$ ) calculated as  $L = 1 - R - T$  are presented in the same figure. Losses due to absorption have a maximum in the spectral range 500-700 nm where  $R_a$  has its minimum. In this case more light can arrive to the MIF and be absorbed there. From the measurements it is possible to see that the experimental curves match the theoretical ones excellently.

The performance of dielectric layers depends on interference and changes with AOI, since optical phase properties are changing. The performance of the presented designs is based mainly on absorption of light that is almost independent on the angle of incidence [9]. However, due to the dielectric layers employed, the performance will not be completely independent on the angle. We have compared angular shifts of TAD91 experimental spectrum and theoretical spectrum of a modified TAD91 design containing only dielectric layers. The performance of the MIF containing system is less sensitive to AOI than the all dielectric one. The maximum of reflectance of the TAD91 sample shifts from 537 to 507 nm and the maximum of all dielectric design shifts from 560 to 520 nm.

**Table 2. Comparison of the desired and obtained colour chromaticities.**

Design	Theoretical colour chromaticities		Experimental colour chromaticities	
	$R_a$	$R_b$	$R_a$	$R_b$
TAD32	$x = 0.23, y = 0.18$	$x = 0.41, y = 0.46$	$x = 0.21, y = 0.11$	$x = 0.47, y = 0.46$
TAD7a	$x = 0.21, y = 0.11$	$x = 0.47, y = 0.45$	$x = 0.22, y = 0.18$	$x = 0.41, y = 0.45$
TAD7b	$x = 0.39, y = 0.20$	$x = 0.46, y = 0.48$	$x = 0.37, y = 0.19$	$x = 0.46, y = 0.49$
TAD8b	$x = 0.46, y = 0.4$	$x = 0.29, y = 0.44$	$x = 0.45, y = 0.41$	$x = 0.26, y = 0.42$
TAD91	$x = 0.27, y = 0.49$	$x = 0.38, y = 0.52$	$x = 0.27, y = 0.48$	$x = 0.38, y = 0.52$

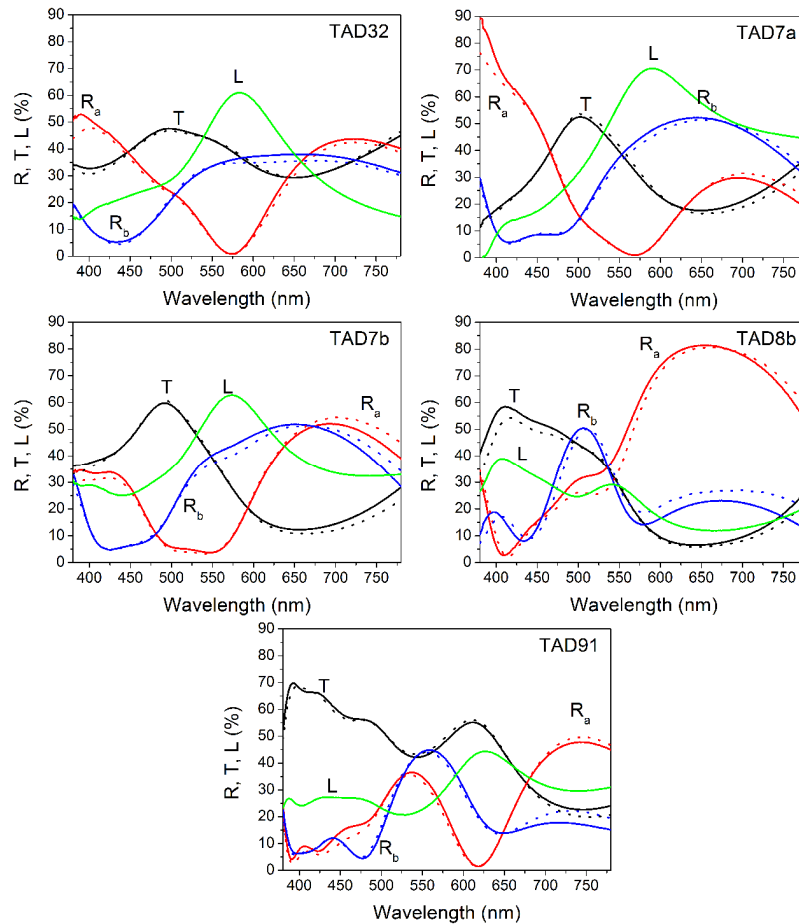


Fig. 3. Experimental (full line) and theoretical (dot) transmittance ( $T$ ), total loss ( $L$ ), reflectance from the front side ( $R_a$ ) and back side ( $R_b$ ) of the samples.

## 5. Conclusions

A set of designs containing metal clusters reflecting different colours from front and back side of the coating was obtained by numerical optimization. This kind of performance is not possible to realize with dielectric coatings only, but a layer of a material absorbing in the range of interest has to be used. Compared to thin compact metal layers, MIFs have lower absorbance and therefore higher transmittances are attainable. They are easy to manufacture and the absorption peak can be tuned easily. The dependence of effective optical constants of a MIF on the quantity of deposited metal was determined from a set of samples containing metal clusters embedded in a dielectric matrix. The chosen designs that were deposited present a variety of achievable colours. Spectrophotometric measurements verified that the produced coatings present excellent agreement with the theoretical optical performance of the designs. Such an agreement verifies that the effective optical constants resulting from MIF characterization enable treating this kind of layer as a standard homogeneous film in the well-established design algorithms. Numerical optimization was verified as a useful method in design of coatings containing MIFs. It should be taken into account that the inclusion of MIFs into numerical optimization software requires knowledge about the thickness dependence of optical constants. We expect that our contribution will make the implementation of metal clusters into multilayer designs easier, enabling obtaining optical coatings with characteristics

that cannot be achieved using standard materials. This would open up the way to novel applications of MIFs.